Supplement of The Cryosphere, 19, 4671–4699, 2025
https://doi.org/10.5194/tc-19-4671-2025-supplement

The Cryosphere Open Access EGU

Supplement of

Quantifying the impacts of atmospheric rivers on the surface energy budget of the Arctic based on reanalysis

Chen Zhang et al.

Correspondence to: Chen Zhang (chen.zhang-3@colorado.edu) and John J. Cassano (john.cassano@colorado.edu)

Introduction

This supporting information provides Supplementary Figures and Tables, organized as follows:

1. Figure S1 provides a map delineating the spatial divisions of four Arctic sub-regions utilized for computing area-averaged results of AR occurrence frequency, surface energy budget (SEB) terms, surface temperature and 2-meter air temperature (T-2m), as presented in Table 1 and Table S1-S3.

2. Figure S2-S3 illustrates the spatial distributions of 40-year mean climatology, mean composite anomalies during the presence of AR events, the total contributions of AR-related anomalies to the climatology, and the relative contributions to the mean SEB during each season, for sensible heat flux (SH) and latent heat flux (LH), respectively.

3. Figure S4 visualizes the 85th percentile climatological threshold of integrated water vapor transport (IVT) in ERA5 for January, spanning from 1980 to 2019. This figure serves as a representative of winter and facilitates the analysis of differences between the 85th_IVT AR index and M24 AR index results.

4. Figure S5-S14 show the results of the statistical significance of AR-induced anomalies at the 95% confidence level, determined using a two-tailed t-test. To account for temporal autocorrelation, we adjust the effective sample size by dividing the total number of AR time steps at a grid point by the average number of time steps during individual AR events, allowing the sample size to reflect distinct AR events at each grid point. Specifically, Figures S5–S14 display AR-induced anomalies for various variables, including surface downward longwave radiation (LWD), net surface longwave radiation (LWN), net surface shortwave radiation (SWN), turbulent heat flux (TH), net SEB, SH, LH, surface temperature, T-2m, and LWD but based on the M24 AR index.

4. Table S1 displays regional average results of the 40-year average climatology, composite anomalies during AR events, the corresponding total contribution to the climatology and to the net SEB, and the extra AR contribution relative to the AR frequency for LWN, SWN, and TH. Symbols indicating the percentage of anomalies within each region at a 95% confidence level determined using a two-tailed t-test with adjusted effective sample size reflecting distinct AR events: one asterisk (*), two asterisks (**), and bolded values with two asterisks (X**) represent >50%, >90%, and >95% of grid points, respectively, as shown in Figs. S6-S8.

5. Table S2 presents the regional average results for the 40-year mean climatology and composite anomalies during AR events for surface temperature and T-2m air temperature. Symbols indicating the percentage of anomalies within each region at a 95% confidence level determined using a two-tailed t-test with adjusted effective sample size reflecting distinct AR events: one asterisk (*), two asterisks (**), and bolded values with two asterisks (X**) represent >50%, >90%, and >95% of grid points, respectively, as shown in Figs. S12-S13.

6. Table S3, based on the M24 AR index, provides the regional results for AR occurrence frequency, LWD anomalies during AR events, the total contributions of these AR LWD anomalies to the LWD climatology, their relative contribution to the mean SEB, along with the extra AR contribution relative to the corresponding AR frequency. Symbols indicating the

percentage of anomalies within each region at a 95% confidence level determined using a two-tailed t-test with adjusted effective sample size reflecting distinct AR events: one asterisk (*), two asterisks (**), and bolded values with two asterisks (X**) represent >50%, >90%, and >95% of grid points, respectively, as shown in Figs. S14.

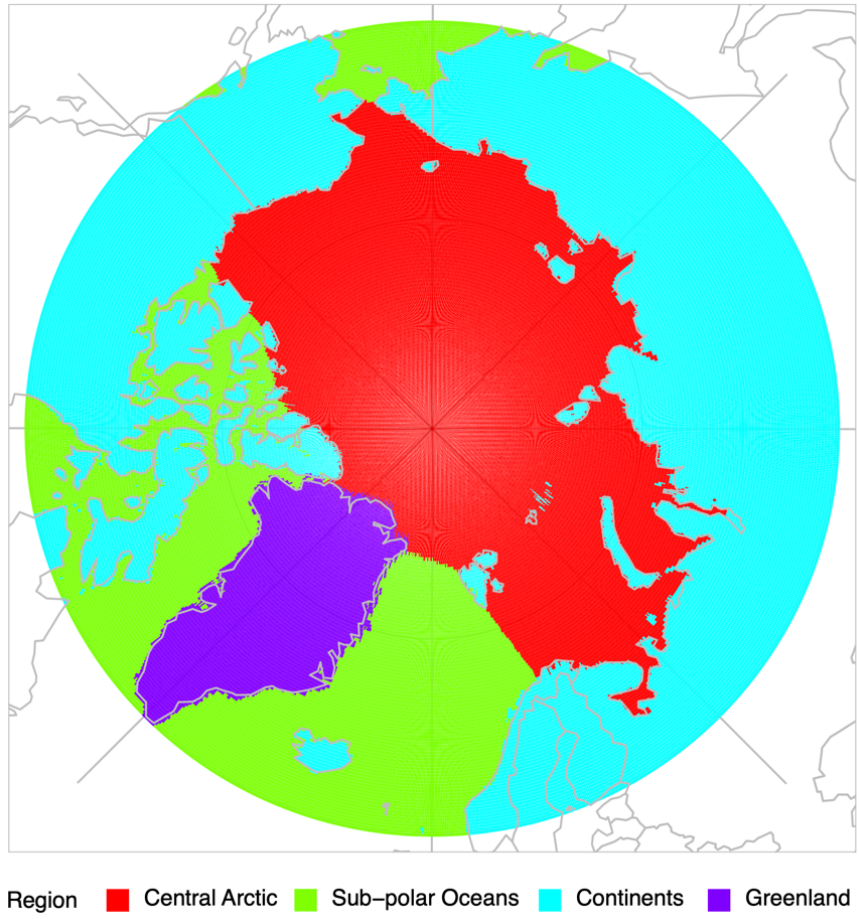

Figure S1. Map showing the spatial division of four sub-regions for calculating area averages of AR occurrence frequency, surface energy budget terms, T-2m and surface temperature, as presented in Table 1 and Table S1-S3. The central Arctic, including the Barents and Kara Seas, is highlighted in red; Sub-polar oceans in green; Continents in cyan; and Greenland in purple.

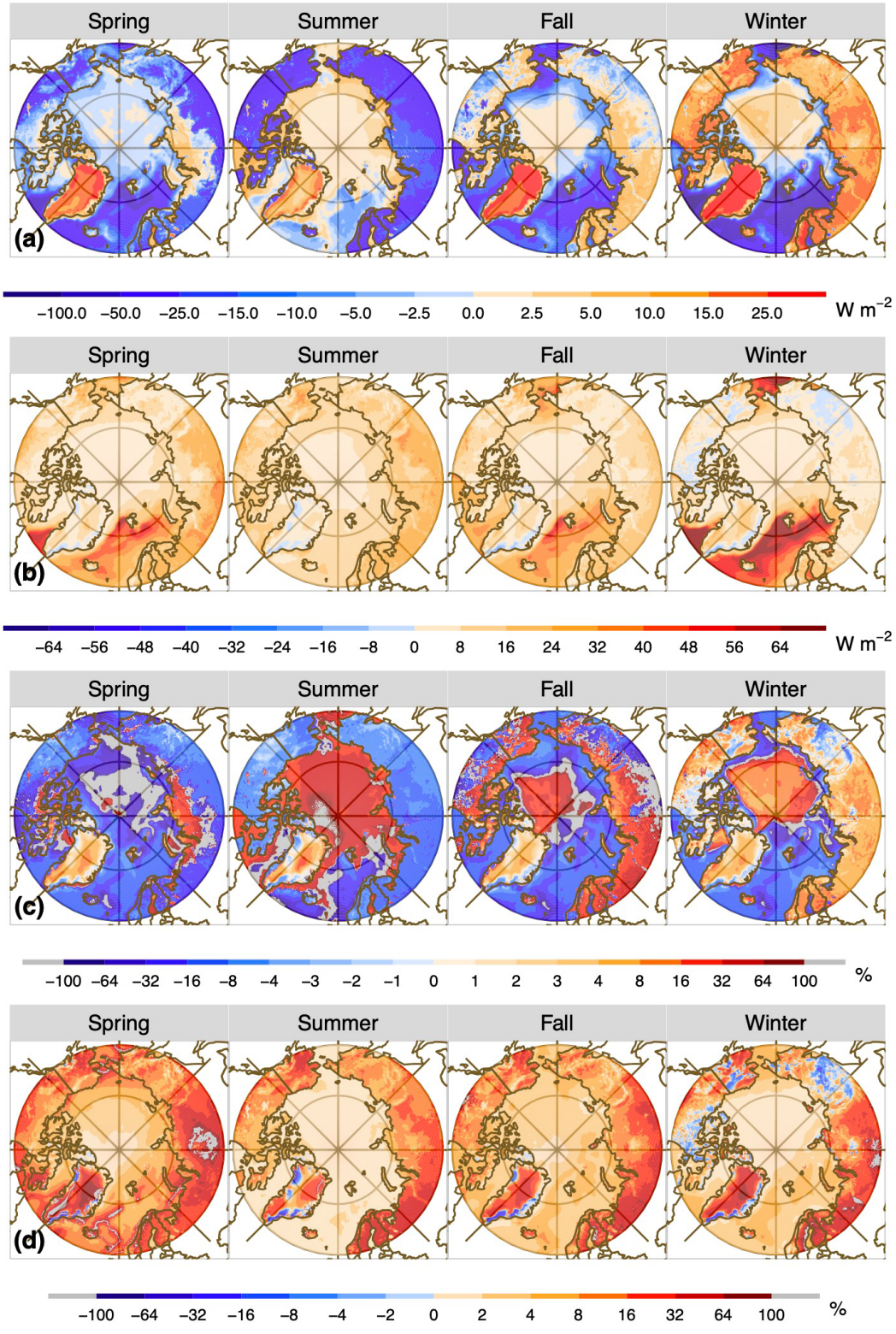
Spring
Summer
Fall
Winter
(a)
−100.0 −50.0 −25.0 −15.0 −10.0 −5.0 −2.5 0.0 2.5 5.0 10.0 15.0 25.0
W m−2
Spring
Summer
Fall
Winter
(b)
−64 −56 −48 −40 −32 −24 −16 −8 0 8 16 24 32 40 48 56 64
W m−2
Spring
Summer
Fall
Winter
(c)
−100 −64 −32 −16 −8 −4 −3 −2 −1 0 1 2 3 4 8 16 32 64 100
%
Spring
Summer
Fall
Winter
(d)
−100 −64 −32 −16 −8 −4 −2 0 2 4 8 16 32 64 100
%

40

Figure S2. Maps showing (a) the spatial distributions of 40-year mean sensible heat flux (SH, unit: W m^{-2}) across spring (March-May), summer (June-August), fall (September-November), and winter (December-February) from 1980 to 2019. (b) Spatial distributions of 40-year mean SH anomalies (unit: W m^{-2}) during the presence of AR events within each season. (c) Spatial distributions of the fraction of the 40-year AR contribution (unit: %) of the total SH anomalies to the SH climatology. (d) Spatial distribution of their relative contribution to the absolute values of 40-year mean SEB for each season. Note that all positive vertical fluxes values directed downwards towards the surface. The percentage results greater than 100% or less than -100% are shaded in grey for clarity.

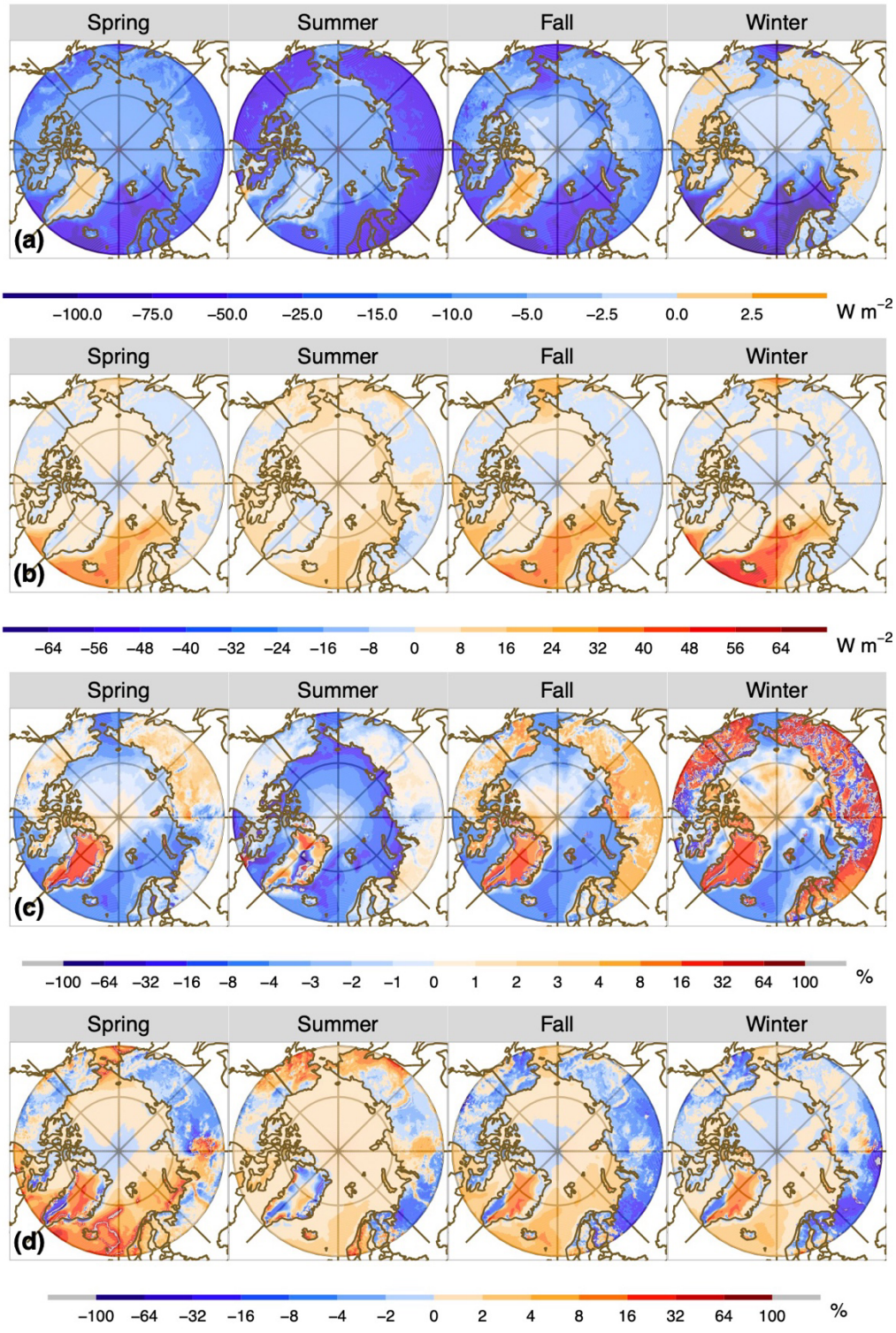

Figure S3. Similar to Figure S2, but for results according to the surface latent heat flux (LH).

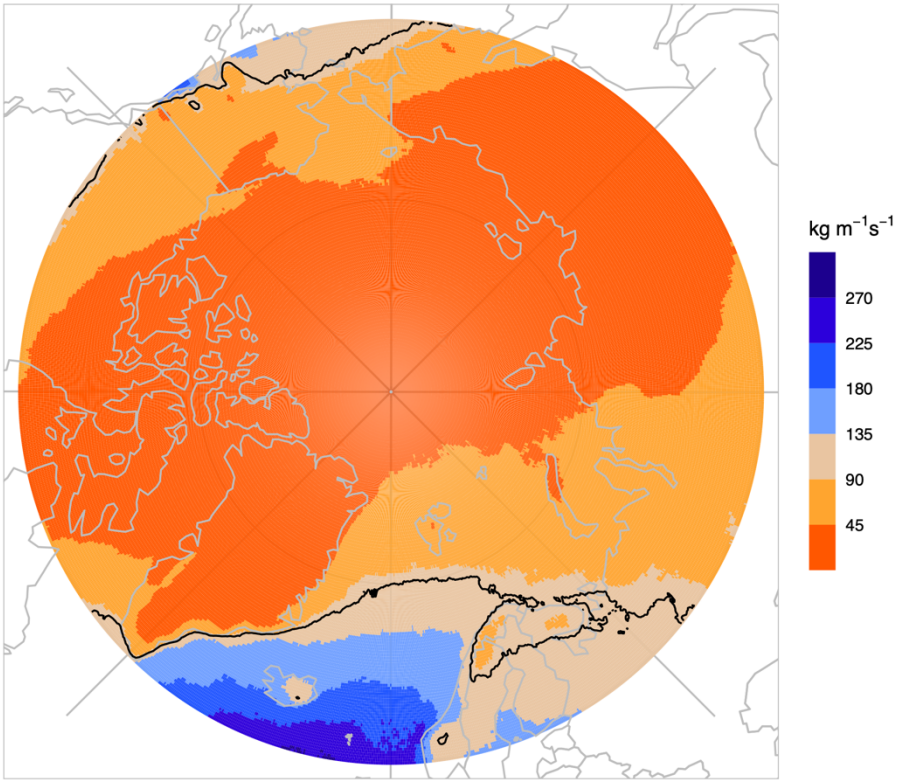

50

Figure S4. The 85th percentile climatological threshold of IVT in ERA5 (unit: kg m^{-1} s^{-1}) for January from 1980 to 2019, the black line is the 100 kg m^{-1} s^{-1} minimum criteria values that the M24 AR detection algorithm applies to complement the 85th percentile climate threshold.

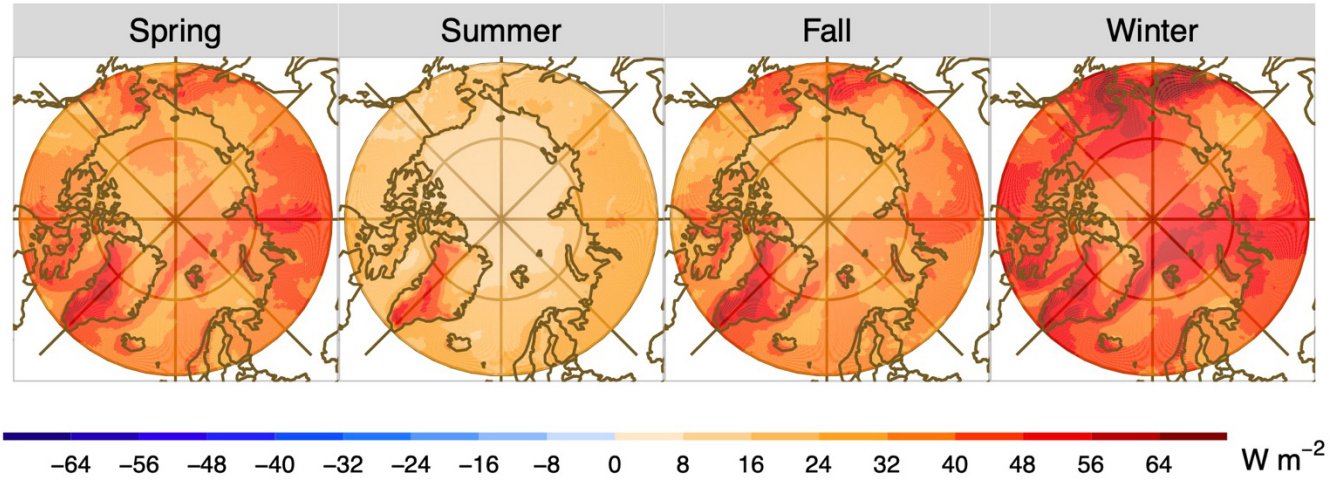

Figure S5. Spatial distributions of 40-year mean surface downward longwave radiation (LWD) anomalies (unit: W m^{-2}) during the presence of AR events within each season: spring (March-May), summer (June-August), fall (September-November), and winter (December-February). The grey dots indicate regions where the anomalies are not statistically significant at the 95% confidence level, based on a two-tailed t-test. In the t-test, the effective sample size is adjusted by reducing the number of total AR time steps to distinct AR events at each grid point to account for temporal autocorrelation.

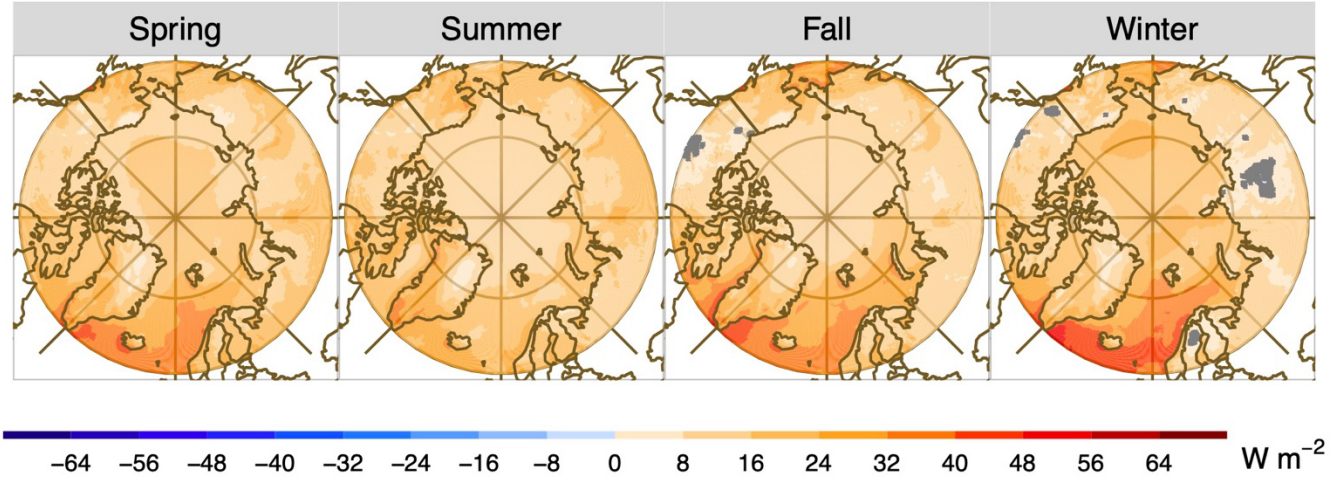

Figure S6. Similar to Figure S5, but for AR-induced net surface longwave radiation (LWN) anomalies (unit: W m^{-2}) within each season. The grey dots indicate regions where the anomalies are not statistically significant at the 95% confidence level, based on a two-tailed t-test. In the t-test, the effective sample size is adjusted by reducing the number of total AR time steps to distinct AR events at each grid point to account for temporal autocorrelation.

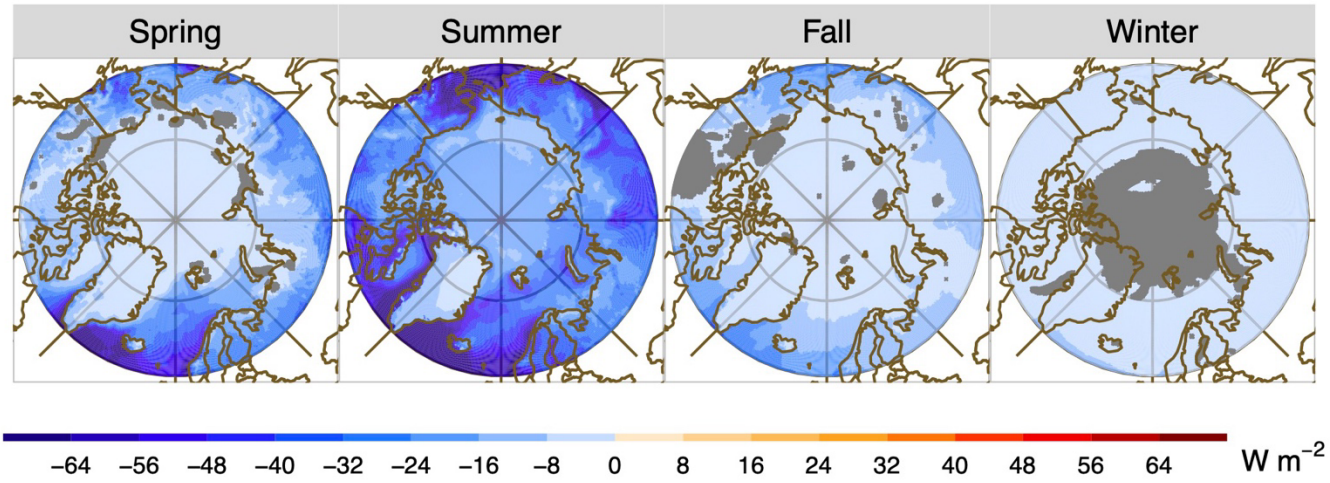

Figure S7. Similar to Figure S5, but for AR-induced surface shortwave radiation (SWN) anomalies (unit: W m^{-2}) within each season. The grey dots indicate regions where the anomalies are not statistically significant at the 95% confidence level, based on a two-tailed t-test. In the t-test, the effective sample size is adjusted by reducing the number of total AR time steps to distinct AR events at each grid point to account for temporal autocorrelation.

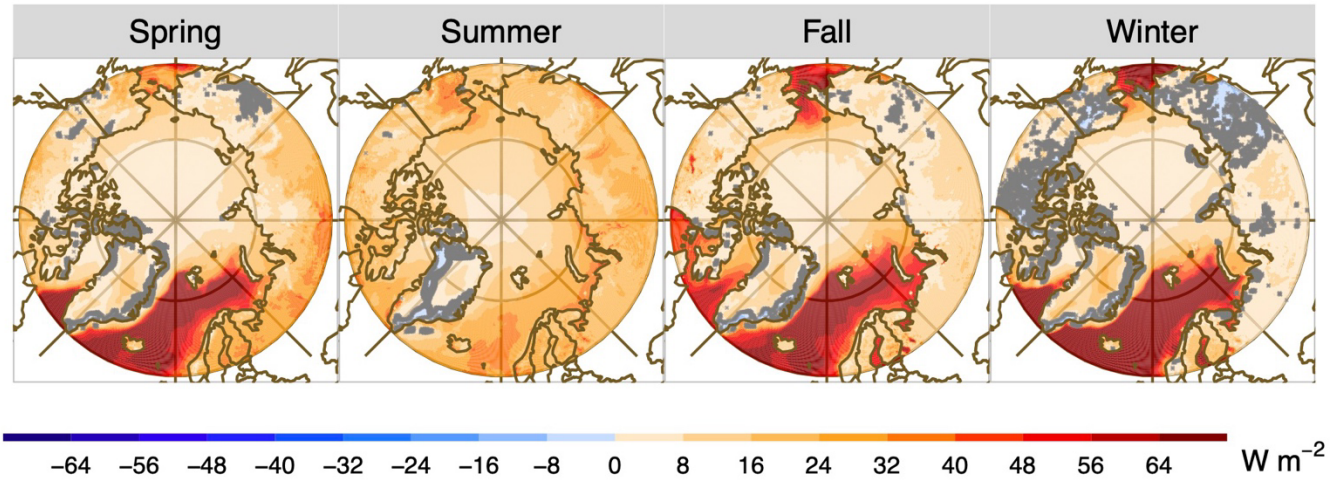

Figure S8. Similar to Figure S5, but for AR-induced turbulent heat flux (TH) anomalies (unit: W m^{-2}) within each season. The grey dots indicate regions where the anomalies are not statistically significant at the 95% confidence level, based on a two-tailed t-test. In the t-test, the effective sample size is adjusted by reducing the number of total AR time steps to distinct AR events at each grid point to account for temporal autocorrelation.

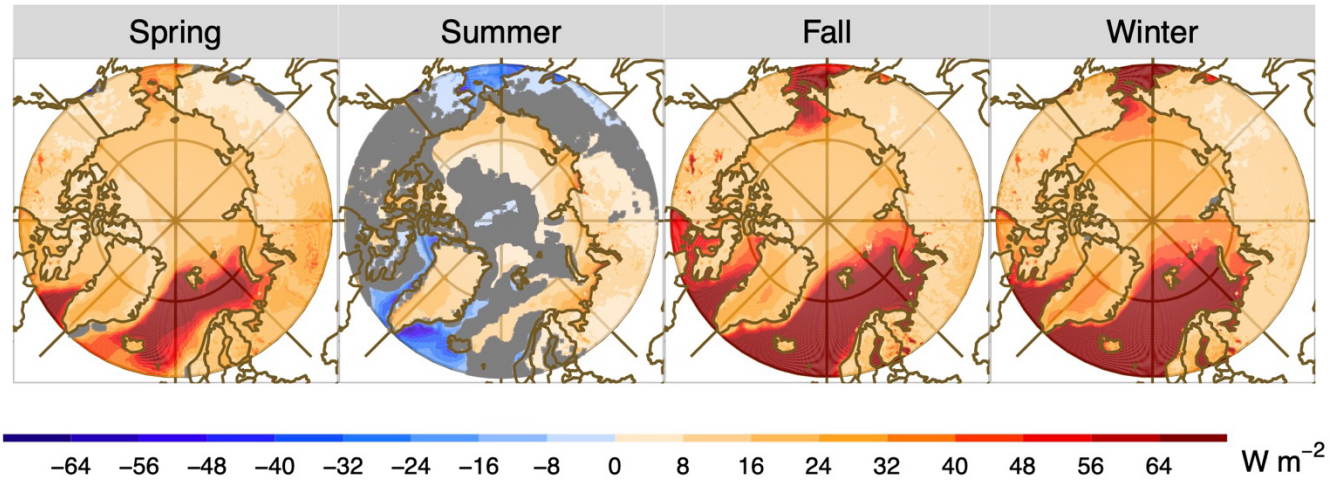

Figure S9. Similar to Figure S5, but for AR-induced net SEB anomalies (unit: W m^{-2}) within each season. The grey dots indicate regions where the anomalies are not statistically significant at the 95% confidence level, based on a two-tailed t-test. In the t-test, the effective sample size is adjusted by reducing the number of total AR time steps to distinct AR events at each grid point to account for temporal autocorrelation.

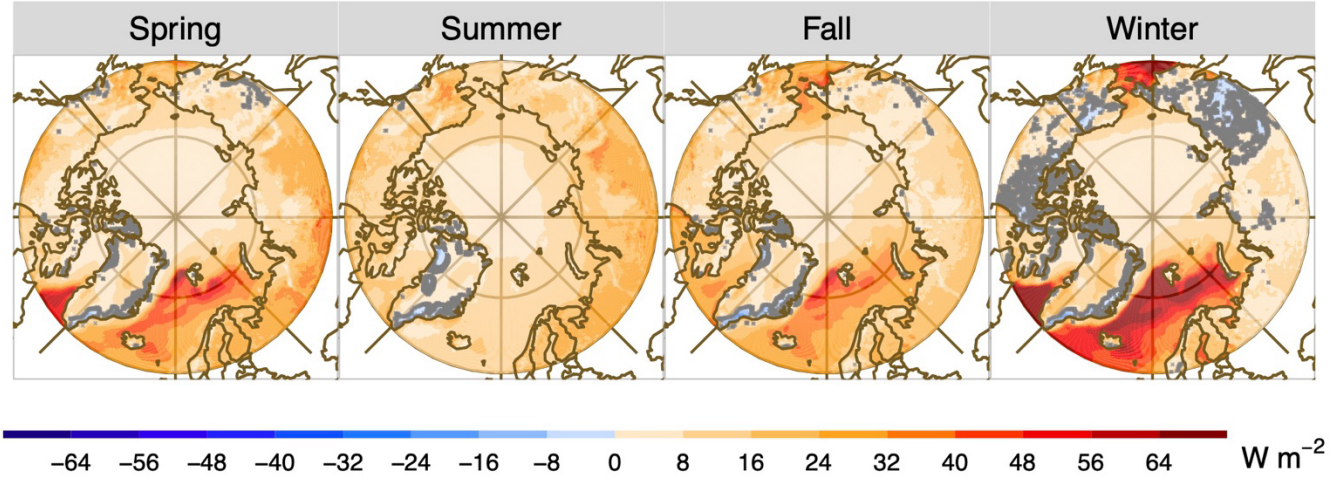

Figure S10. Similar to Figure S5, but for AR-induced sensible heat flux (SH) anomalies (unit: W m^{-2}) within each season. The grey dots indicate regions where the anomalies are not statistically significant at the 95% confidence level, based on a two-tailed t-test. In the t-test, the effective sample size is adjusted by reducing the number of total AR time steps to distinct AR events at each grid point to account for temporal autocorrelation.

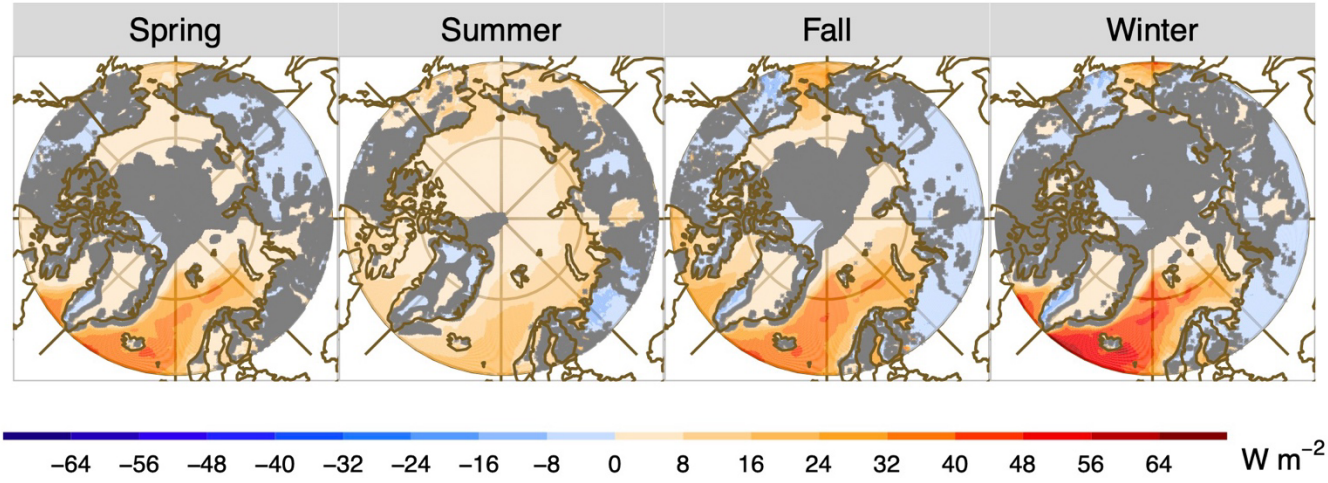

Figure S11. Similar to Figure S5, but for AR-induced latent heat flux (LH) anomalies (unit: W m^{-2}) within each season. The grey dots indicate regions where the anomalies are not statistically significant at the 95% confidence level, based on a two-tailed t-test. In the t-test, the effective sample size is adjusted by reducing the number of total AR time steps to distinct AR events at each grid point to account for temporal autocorrelation.

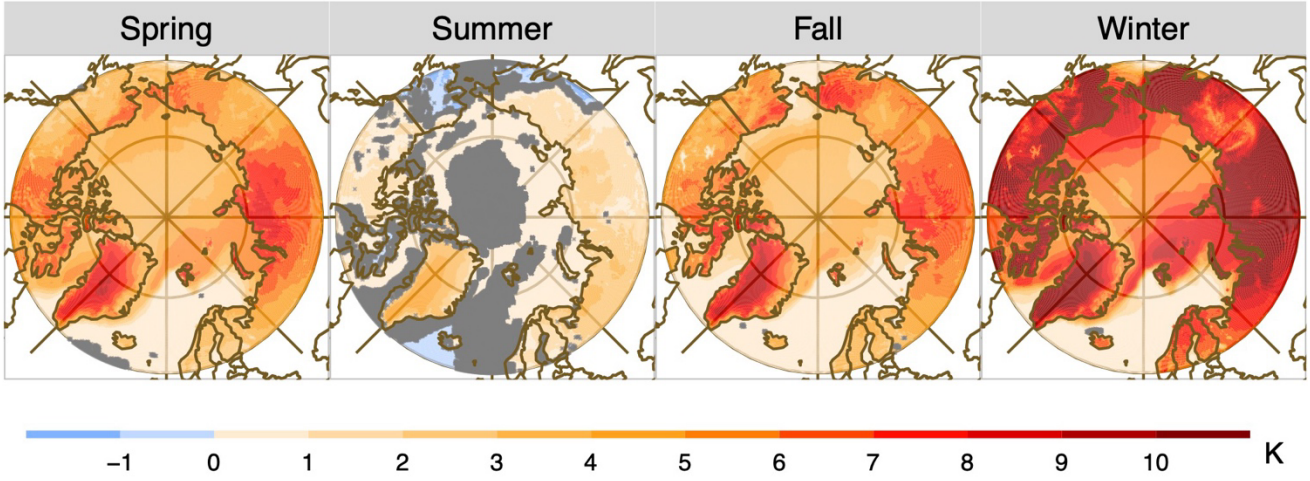

Figure S12. Spatial distributions of 40-year mean surface temperature anomalies (unit: K) during the presence of AR events within each season: spring (March-May), summer (June-August), fall (September-November), and winter (December-February). The grey dots indicate regions where the anomalies are not statistically significant at the 95% confidence level, based on a two-tailed t-test. In the t-test, the effective sample size is adjusted by reducing the number of total AR time steps to distinct AR events at each grid point to account for temporal autocorrelation.

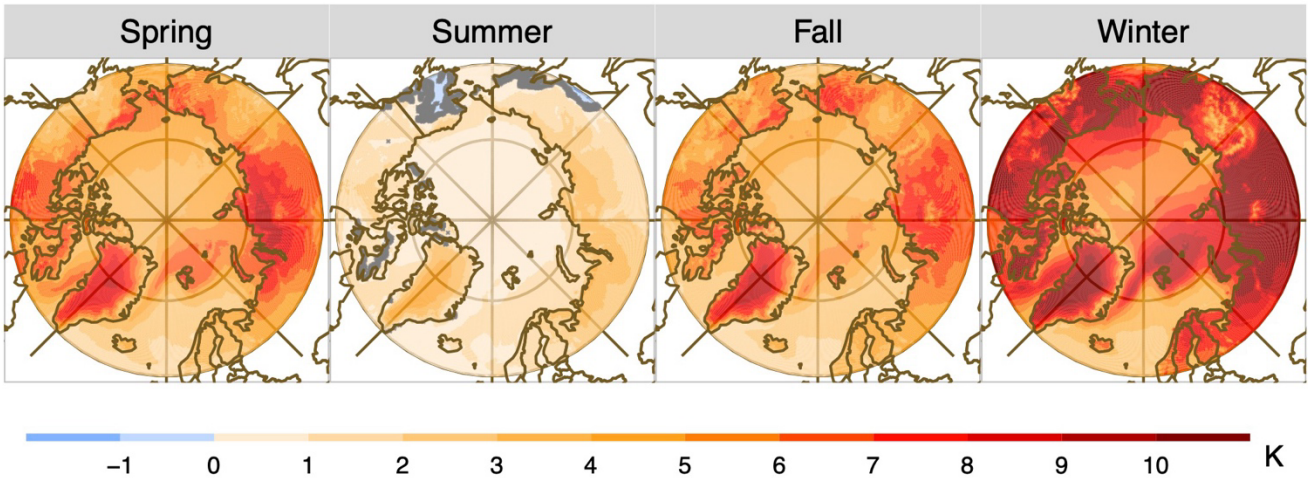

Figure S13. Similar to Figure S12, but for AR-induced T-2m air temperature anomalies (unit: K) within each season. The grey dots indicate regions where the anomalies are not statistically significant at the 95% confidence level, based on a two-tailed t-test. In the t-test, the effective sample size is adjusted by reducing the number of total AR time steps to distinct AR events at each grid point to account for temporal autocorrelation.

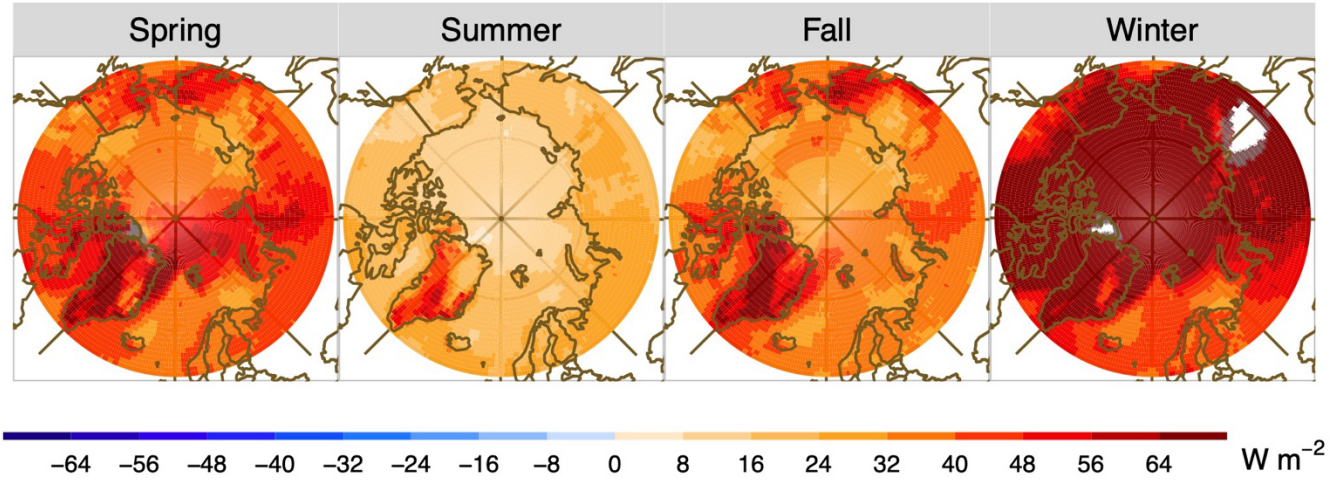

Figure S14. According to M24 AR detection index, spatial distributions of 40-year mean surface downward longwave radiation (LWD) anomalies (unit: W m^{-2}) during the presence of AR events within each season: spring (March-May), summer (June-August), fall (September-November), and Winter (December-February). The grey dots indicate regions where the anomalies are not statistically significant at the 95% confidence level, based on a two-tailed t-test. In the t-test, the effective sample size is adjusted by reducing the number of total AR time steps to distinct AR events at each grid point to account for temporal autocorrelation.

Surface Net Longwave Radiation (LWN)								
Region	Central Arctic	Subpolar Oceans	Continents	Greenland	Central Arctic	Subpolar Oceans	Continents	Greenland

Season	Spring				Summer			
AR Freq. (%)	10.8	12.3	12.2	12.2	10.4	11.8	11.6	11.1
Climatology (W m^{-2})	-39.5	-50.3	-47.3	-47.5	-23.2	-34.4	-53.4	-51.3
Anomalies (W m^{-2})	**17.1****	**27.4****	**16.6****	**20.4****	**13.8****	**21.1****	**17****	**22.1****
Cotrib. to climo (%)	-4.7	-6.7	-4.5	-5.4	-6.3	-7.4	-3.9	-5
Cotrib. to SEB (%)	20.8	49.3	95.1	2618.8	2.2	2.6	13.2	101.9
Extra AR (%)	10	37	82.9	2606.6	-8.2	-9.2	1.6	90.8
Season	**Fall**				**Winter**			
AR Freq. (%)	10.6	12.4	12.5	11.8	10.5	12.3	12.7	12.4
Climatology (W m^{-2})	-33.6	-50.7	-34.9	-39.2	-43.8	-56.3	-27.1	-37.7
Anomalies (W m^{-2})	**16.2****	**29.9****	**13.9****	**20.8****	**21.8****	**31.2****	**11.5****	**18.1****
Cotrib. to climo (%)	-5.1	-7.3	-5.1	-6.5	-5.2	-6.8	-5.7	-6.8
Cotrib. to SEB (%)	4.2	4.6	19.6	41.8	4.4	3.3	41.3	52
Extra AR (%)	-6.4	-7.8	7.1	30	-6.1	-9	28.6	39.6

Surface Net Shortwave Radiation (SWN)								
Region	**Central Arctic**	**Subpolar Oceans**	**Continents**	**Greenland**	**Central Arctic**	**Subpolar Oceans**	**Continents**	**Greenland**
Season	**Spring**				**Summer**			
AR Freq. (%)	10.8	12.3	12.2	12.2	10.4	11.8	11.6	11.1
Climatology (W m^{-2})	36.4	86.1	81.8	34.8	99.9	153.8	156.6	64.9
Anomalies (W m^{-2})	**-6.2****	**-29.4****	**-16.5****	**-7.5****	**-22.0****	**-52.0****	**-34.5****	**-17.4****
Cotrib. To climo (%)	-1.8	-3.8	-2.5	-2.4	-2.3	-3.9	-2.6	-2.6
Cotrib. to SEB (%)	-7.7	-50.7	-66.6	-553.6	-3.5	-6.2	-27.3	-46.6
Extra AR (%)	-3.1	38.4	54.4	541.4	-6.9	-5.6	15.7	35.5
Season	**Fall**				**Winter**			
AR Freq. (%)	10.6	12.4	12.5	11.8	10.5	12.3	12.7	12.4
Climatology (W m^{-2})	10.9	33	31	9.7	0.4	5.6	5.8	1.1
Anomalies (W m^{-2})	**-2.6****	**-14.4****	-8.3**	**-3.3****	-0.1	-2.3*	-1.5**	-0.4*
Cotrib. To climo (%)	-2.5	-5.1	-3.4	-3.3	-2	-4.3	-3.3	-2.9
Cotrib. to SEB (%)	-0.6	-2.2	-12.3	-4.7	0	-0.2	-7.8	-0.5
Extra AR (%)	-10	-10.2	-0.2	-7.1	-10.5	-12.1	-4.9	-11.9

Turbulent Heat Flux (TH)								
Region	**Central Arctic**	**Subpolar Oceans**	**Continents**	**Greenland**	**Central Arctic**	**Subpolar Oceans**	**Continents**	**Greenland**
Season	**Spring**				**Summer**			
AR Freq. (%)	10.8	12.3	12.2	12.2	10.4	11.8	11.6	11.1
Climatology (W m^{-2})	-16.5	-57.5	-25.2	13.1	-7	-15.5	-81.3	-0.9
Anomalies (W m^{-2})	**14.9****	**41.8****	**15.1****	7.1*	**17.1****	**22.9****	**20.7****	5.6*
Cotrib. To climo (%)	-23.6	-11.4	36.7	3.5	163.3	-6.6	6.3	-2.6
Cotrib. to SEB (%)	18.7	66.8	61	134	2.5	2.8	16.8	7.2
Extra AR (%)	7.9	54.5	48.8	121.8	-7.9	-9	5.2	-3.9
Season	**Fall**				**Winter**			
AR Freq. (%)	10.6	12.4	12.5	11.8	10.5	12.3	12.7	12.4
Climatology (W m^{-2})	-25.3	-72.2	-9.1	18.1	-21.3	-96.2	11.2	23.8
Anomalies (W m^{-2})	**20.8****	**48.6****	**10.4****	7.4*	**17.5****	**62.1****	5.6*	10*
Cotrib. To climo (%)	-31.1	-9.2	-8.6	2.5	-9.8	-8.3	6.8	2.9
Cotrib. to SEB (%)	4.3	7	16.3	17.3	2.5	4.8	16.4	28
Extra AR (%)	-6.3	-5.4	3.8	5.5	-8	-7.5	3.7	15.6

Table S1. Regional average results of net surface longwave radiation (LWN, top part), net surface shortwave radiation (SWN, middle part) and turbulent heat flux (TH, bottom part) across different seasons: spring, summer, fall, and winter. Results include AR occurrence frequency (AR Freq., unit: %), Climatology (unit: W m^{-2}), composite anomalies (unit: W m^{-2}), total AR contribution to respective climatology (Cotrib. To climo, unit: %), and relative contribution to absolute net SEB (Cotrib. to SEB, unit: %), and relative AR contribution to the net SEB compared to the AR frequency (Extra AR, unit: %). Symbols indicating the percentage of anomalies within each region at a 95% confidence level determined using a two-tailed t-test with adjusted effective sample size reflecting distinct AR events: one asterisk (*), two asterisks (**), and bolded values with two asterisks (X) represent >50%, >90%, and >95% of grid points, respectively, as shown in Figs. S6, S7 and S8.**

Surface Temperature								
Region	**Central Arctic**	**Subpolar Oceans**	**Continents**	**Greenland**	**Central Arctic**	**Subpolar Oceans**	**Continents**	**Greenland**
Season	**Spring**				**Summer**			
AR Freq. (%)	10.8	12.3	12.2	12.2	10.4	11.8	11.6	11.1
Climatology (K)	259.8	269.4	263.6	250.3	274.2	278.4	284	266.4
Anomalies (K)	**4****	**2.1****	**5.2****	**6.4****	0.1	0.03	1.1*	2.8**

Season	Fall				Winter			
AR Freq. (%)	10.6	12.4	12.5	11.8	10.5	12.3	12.7	12.4
Climatology (K)	264.7	274.9	265.4	251.6	252.3	265.9	247.5	242.4
Anomalies (K)	**3.1****	**1.1****	**5.4****	**7****	**6.2****	**3.2****	**9.5****	**8.6****
T-2m Air Temperature								
Region	Central Arctic	Subpolar Oceans	Continent	Greenland	Central Arctic	Subpolar Oceans	Continents	Greenland
Season	Spring				Summer			
AR Freq. (%)	10.8	12.3	12.2	12.2	10.4	11.8	11.6	11.1
Climatology (K)	259.5	268.2	264.3	253	274.5	278.6	283.8	267.9
Anomalies (K)	**4.5****	**3.5****	**5.7****	**6.5****	**0.8****	**0.9****	1.7**	**2.9****
Season	Fall				Winter			
AR Freq. (%)	10.6	12.4	12.5	11.8	10.5	12.3	12.7	12.4
Climatology (K)	264	273.4	266.2	254.9	251.8	263.8	249	246.5
Anomalies (K)	**4****	**2.8****	**5.6****	**6.7****	**6.8****	**5.2****	**9.4****	**8.3****

Table S2. Regional average results of Surface Temperature (top panel) and T-2m Air Temperature (bottom panel) across different seasons: Spring, Summer, Fall, and Winter. Results include AR occurrence frequency (AR Freq., unit: %), Climatology (unit: K), composite anomalies (unit: K). Symbols indicating the percentage of anomalies within each region at a 95% confidence level: one asterisk (*), two asterisks (**), and bolded values with two asterisks (X) represent >50%, >90%, and >95% of grid points, respectively, as shown in Figs. S12 and S13.**

Surface Downward Longwave Radiation (LWD)								
Region	Central Arctic	Subpolar Ocean	Continents	Greenland	Central Arctic	Subpolar Ocean	Continents	Greenland
Season	Spring				Summer			
AR Freq. (%)	1.7	5.5	3.1	2.1	7.7	8.6	8.3	5.4
Anomalies (W m^{-2})	**40.8****	**43.6****	**44.2****	**61.5****	**13.7****	**22****	**22.5****	**37.9****
Cotrib. to climo (%)	0.3	0.9	0.6	0.7	0.4	0.6	0.6	0.9
Cotrib. to SEB (%)	7.2	39.4	78.7	373	1.6	1.9	13	54.5
Extra AR (%)	5.5	33.9	75.6	370.9	-6.1	-6.7	4.7	49.1
Season	Fall				Winter			
AR Freq. (%)	3.1	7.4	4.9	3.4	1.3	6	2.3	1.6

Anomalies (W m^{-2})	31.1**	38.1**	38.2**	60.4**	73.4**	59.9**	65.9**	76.8**
Cotrib. to climo (%)	0.4	1	0.7	1	0.4	1.1	0.6	0.7
Cotrib. to SEB (%)	2.2	3.4	22.6	34.7	1.2	2	32.7	16.6
Extra AR (%)	-0.9	-3.6	17.7	31.3	-0.1	-4	30.4	15

Table S3. According to M24 AR index, regional average results of AR occurrence frequency (AR Freq., unit: %), composite anomalies of Surface Downward Longwave Radiation (LWD) during AR events (Anomalies, unit: W m^{-2}), total AR contribution to the respective climatology (Contrib. to climo, unit: %) and total AR contribution to absolute net SEB (Contrib. to SEB, unit: %), and relative AR contribution to the net SEB compared to the AR frequency (Extra AR, unit: %) across different seasons: spring, summer, fall, and winter. Symbols indicating the percentage of anomalies within each region at a 95% confidence level: one asterisk (*), two asterisks (**), and bolded values with two asterisks (X) represent >50%, >90%, and >95% of grid points, respectively, as shown in Fig. S14.**